Impact of the nuclear EoS on fusion *vs.* quasifission processes

M. COLONNA[1], H. ZHENG[2][1], S. BURRELLO[1], D. LACROIX[3] and G. SCAMPS[4]

[1] *INFN, Laboratori Nazionali del Sud - Catania, Italy*
[2] *School of Physics and Information Technology, Shaanxi Normal University - Xi'an 710119, China*
[3] *Institut de Physique Nucléaire, IN2P3-CNRS, Université Paris-Sud, Université Paris-Saclay - F-91406 Orsay Cedex, France*
[4] *Center for Computational Sciences, University of Tsukuba - Tsukuba 305-8571, Japan*

Summary. — Within the Time Dependent Hartree Fock (TDHF) approach, we investigate the impact of several ingredients of the nuclear effective interaction, such as incompressibility, symmetry energy, effective mass, derivative of the Lane potential and surface terms on the exit channel (fusion *vs.* quasifission) observed in the reaction ^{238}U + ^{40}Ca, close to the Coulomb barrier. Our results show that all the ingredients listed above contribute to the competition between fusion and quasifission processes, however the leading role in determining the outcome of the reaction is played by incompressibility, symmetry energy and the isoscalar coefficient of the surface term.

1. – Introduction

Understanding the dissipation mechanisms occurring in low-energy heavy-ion collisions represents one of the most challenging problems in nuclear reaction and structure studies [1-3]. Crucial information is provided by the investigation of strongly damped collisions of nuclei, that may lead to (incomplete) fusion, quasifission or deep-inelastic processes. In particular, dissipative reaction dynamics plays an essential role in the synthesis of superheavy elements (SHE), a quite appealing challenge of modern nuclear physics [4-6].

At low energies (close and/or above the Coulomb barrier), heavy-ion reactions are governed, to a large extent, by one-body dissipation mechanisms (see for instance [7]). From a microscopic point of view, their description can be addressed within the Time Dependent Hartree Fock (TDHF) approach [4,8-11], and its semi-classical approximation (the Vlasov equation), see the recent refs. [12,13] and references therein. These mean-field approaches (including stochastic extensions, that account for quantum fluctuations) provide a suitable framework to study the many-body system at a fully microscopic

level and have been successfully applied to describe fusion reactions, nucleon transfer and deep inelastic collisions, as well as the quasifission dynamics [11]. Apart from the expected sensitivity to the properties, such as charge, mass and deformation, of the two colliding nuclei, the reaction path is quite influenced also by the ingredients of the nuclear effective interaction employed in the calculations. It should be noticed that the latter is closely connected to the nuclear Equation of State (EoS), which plays an important role in nuclear structure, dynamics of heavy ion collisions at intermediate energy and astrophysical phenomena as well.

In this paper, we aim at getting a deeper understanding of the interplay between fusion and quasifission processes in low-energy heavy-ion collisions. As stressed above, this is particularly important in the search of new SHE. In keeping with the spirit of previous studies [14, 13], we investigate, within the TDHF approach, the impact of relevant ingredients of the nuclear effective interaction, such as incompressibility, symmetry energy, effective mass, Lane potential derivative, and surface terms, on the exit channel (fusion *vs.* quasifission) of central heavy-ion reactions close to the Coulomb barrier. Our goal is to establish possible connections between the reaction dynamics and global nuclear matter properties, in density regions around and below the saturation value.

2. – Theoretical description and effective interactions

In the TDHF theory, the evolution of the one-body density matrix $\hat{\rho}(t)$ is determined by

$$(1) \qquad\qquad i\hbar\partial_t\hat{\rho}(t) = [h[\hat{\rho}], \hat{\rho}(t)],$$

where $h[\hat{\rho}] = \mathbf{p}^2/2m + U[\mathbf{p}, \rho]$ is the mean-field Hamiltonian with U as the self-consistent potential and $\rho(\mathbf{r})$ denoting the local density. Within the Density Functional Theory, the starting point is the energy density functional $\mathcal{E}[\rho]$, from which the corresponding nuclear EoS and the potential U can be consistently derived.

In the present work, we adopt Skyrme effective interactions, which are characterized in terms of nine interaction parameters $(t_0, t_1, t_2, t_3, x_0, x_1, x_2, x_3, \sigma)$, plus the spin-orbit coupling constants $W_{0(i)}$ [15]. Apart from the spin-orbit term, the energy density is expressed in terms of the isoscalar, $\rho = \rho_n + \rho_p$, and isovector, $\rho_3 = \rho_n - \rho_p$, densities and kinetic energy densities ($\tau = \tau_n + \tau_p, \tau_3 = \tau_n - \tau_p$) as [13]

$$\mathcal{E}[\rho] \equiv \mathcal{E}_{kin}(\tau) + \mathcal{E}_{pot}(\rho, \rho_3, \tau, \tau_3) = \frac{\hbar^2}{2m}\tau + C_0\rho^2 + D_0\rho_3^2 + C_3\rho^{\sigma+2} + D_3\rho^\sigma\rho_3^2$$
$$(2) \qquad + C_{eff}\rho\tau + D_{eff}\rho_3\tau_3 + C_{surf}(\bigtriangledown\rho)^2 + D_{surf}(\bigtriangledown\rho_3)^2,$$

where the coefficients $C_{..}$, $D_{..}$ are combinations of the standard Skyrme parameters. The Coulomb interaction is also considered in the calculations. It turns out to be useful to explicit the relations between the coefficients of the Skyrme interaction and relevant nuclear properties. In analogy with the studies of ref. [16], we will consider: saturation density ρ_0; energy per nucleon of symmetric nuclear matter at ρ_0 (E_0); incompressibility K_0; isoscalar effective mass m_s^* and isovector effective mass m_v^* at saturation density; symmetry energy at ρ_0 (J); slope of the symmetry energy at ρ_0 (L); strength of the isoscalar surface term $G_S = C_{surf}/2$ and strength of the isovector surface term $G_V = -D_{surf}/2$.

By this connection, it becomes straightforward to explore the impact of specific nuclear matter properties on the reaction dynamics. Here, instead of the isovector effective mass, we prefer to employ the derivative, with respect to the momentum p, of the Lane potential, $U_{Lane} = \frac{U_n - U_p}{2I}$ (being I the asymmetry paramter), which has a more intuitive physical meaning, related to the splitting of neutron and proton effective masses, m_n^* and m_p^*. Thus we introduce the parameter f_I, according to the following relation: $\frac{\mathrm{d}U_{Lane}}{\mathrm{d}p} = \frac{f_I}{m}p$. In our study, we will consider the recently introduced SAMi-J Skyrme effective interactions [17]. According to the strength of the momentum-dependent terms, these interactions lead to an effective isoscalar nucleon mass $m_s^* = 0.675\,m$ and a neutron-proton effective mass splitting $m_n^* - m_p^* = 0.023\,mI$ MeV at saturation density, with the corresponding parameter $f_I = -0.0251$. It should be noticed that the SAMi-J interactions exhibit a correlation between J and L, so that all interactions lead to the same value of the symmetry energy below normal density (at $\rho \approx 0.6\rho_0$), well describing the ground-state properties of nuclei. For neutron-rich nuclei, the interactions with a larger L (and J) value predict a thicker neutron skin.

3. – Results and discussions

We have performed TDHF calculations for the system ^{238}U + ^{40}Ca, at $E_{cm} = 203$ MeV and zero impact parameter. This reaction has been investigated in great detail, for a specified EoS and in the TDHF framework, in previous papers [9,18], that we will consider as a reference for our study. The beam energy considered is in the range of the transition from fusion to quasifission processes, thus it is well adapted to our study of the competition between the two reaction mechanisms. Since the ground state of ^{238}U is deformed, it is worthwhile to consider reaction configurations corresponding to two possible projectile-target orientations: side and tip. For the tip orientation, at the energy considered, quasifission is always observed in TDHF calculations [9-11]. Thus we will concentrate on side collisions in our study. The trajectory of the reaction is traced by evaluating the quadrupole moment $Q_2(t) = \langle 2x^2 - y^2 - z^2 \rangle$ of the composite system, with x denoting the beam axis. An increasing trend of $Q_2(t)$ indicates that the system is evolving towards quasifission. On the other hand, if $Q_2(t)$ stays around a constant value, then the system fuses. To check the outcome of the reaction, one can also look directly at density contour plots at different time instants. One can see that the quasifission happens in a few zs which is consistent with the statements in refs. [9-11].

In fig. 1 (left panel), the time evolution of the quadrupole moment of the composite system is shown for calculations corresponding to three different SAMi-J interactions, namely SAMi-J27, SAMi-J31 and SAMi-J35, whose label denotes the symmetry energy value (J) at saturation density. Clearly, we can see that the SAMi-J35 parametrization leads to quasifission, whereas the other two SAMi-J EoS are associated with fusion. Corresponding density contour plots are shown in fig. 2 for SAMi-J31 and SAMi-J35, respectively, in order to better display this dual behavior. The results shown on fig. 1 (left) would indicate that a larger symmetry energy slope, which results in a thicker neutron skin for neutron rich nuclei, makes the reaction system easier to separate. However, as we will discuss in the following, the three parameterizations also differ by other aspects.

To test the sensitivity of the reaction path to the different ingredients of the effective interaction, we have extended our study (see ref. [19]) enlarging the set of Skyrme interactions employed in the TDHF calculations. In addition to the three SAMi-J parametrizations, we will consider interactions corresponding to the variations of six quantities, with
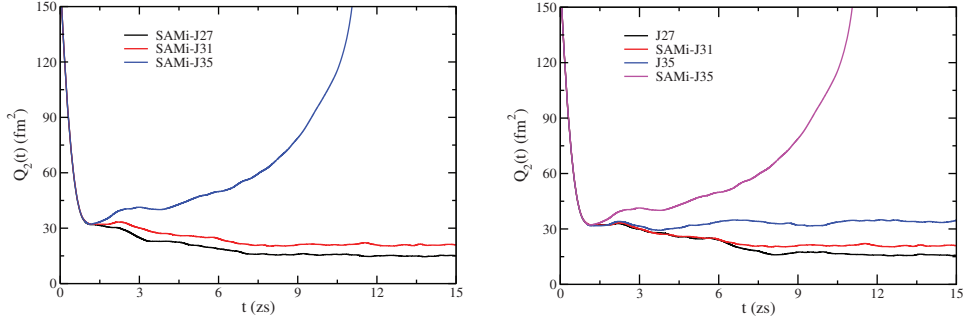
Fig. 1. – Left panel: the quadrupole moment time evolution of the reaction ^{238}U + ^{40}Ca (side orientation) at $E_{cm} = 203$ MeV and $b = 0$ fm, for three SAMi-J EoS. Right panel: the symmetry energy dependence of the quadrupole moment evolution of the reaction considered.

respect to the SAMi-J31, that is taken as a reference: the symmetry energy slope L (keeping the J-L correlation discussed above), the incompressibility, the effective mass, the parameter f_I and the surface terms G_S and G_V. ρ_0 and E_0 are adopted from SAMi-J31 for all the EoS. The EoS name follows the convention that we only label the terms which are different, with respect to the ingredients of the SAMi-J31 parametrization.

3˙1. *Symmetry energy effects*. – In fig. 1 (right panel), we show the quadrupole moment evolution of the reaction considered, for calculations employing the EoS obtained by varying only the symmetry energy properties. One can notice that the result differs from what is shown in the left panel, where the three SAMi-J parametrizations are compared. Indeed SAMi-J35 calculations lead to quasifission, where the J35 parametrization does not, though it presents the same symmetry energy features. This can be explained by considering that the three SAMi-J EoS are characterized not only by a different (J-L) combination, but also exhibit different surface properties. Thus that surface terms play a very important role in the reaction dynamics, as we will discuss in the following section.

3˙2. *Surface term effects*. – In fig. 3 (left), we show the time evolution of the quadrupole moment Q_2, as obtained for the EoS corresponding to different surface term (G_S and G_V) combinations. As is shown in panel (a), by comparing the results associated with
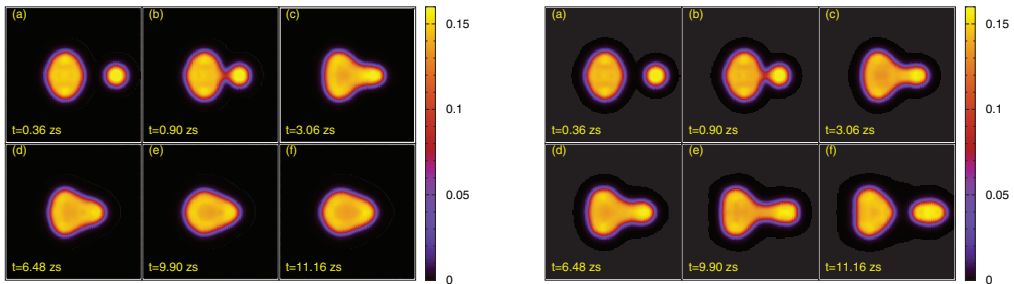

Fig. 2. – Density contour plot at different time instants for the side collision of the reaction ^{238}U + ^{40}Ca (side orientation) at $E_{cm} = 203$ MeV and $b = 0$ fm. The SAMi-J31 (left) and SAMi-J35 (right) interactions are employed.
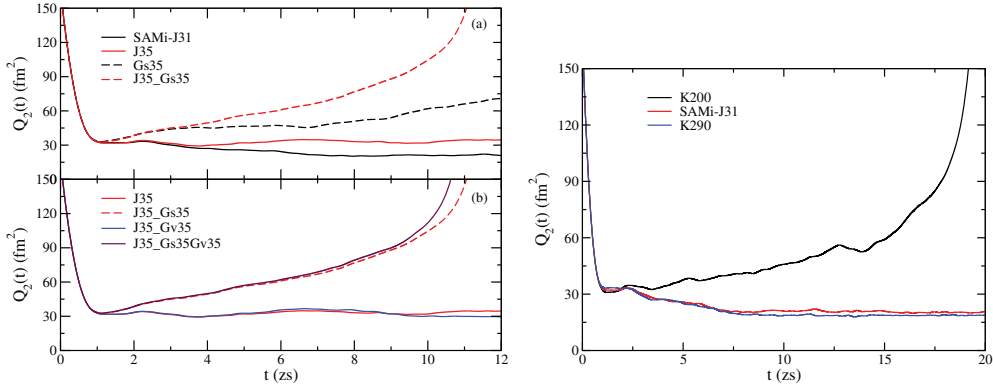
Fig. 3. – Left panels: surface effects on the quadrupole moment evolution of the reaction considered (same as in fig. 1). Right panel: the incompressibility dependence of the quadrupole moment evolution. All reactions are performed at $E_{cm} = 203\,\mathrm{MeV}$ and $b = 0\,\mathrm{fm}$.

SAMi-J31 and Gs35, the reduced G_S surface term of Gs35 helps the system to separate. Combined with a larger symmetry energy (J35), the surface term reduction leads to a quite fast quasifission dynamics (J35_Gs35). This result can be explained considering that, along the approaching phase a reduced surface term favors the formation of more elongated configurations, helping fission. On the other hand, by considering interactions where also G_V is changed significantly, panel (b) shows that the isovector surface term has only a tiny effect on the reaction dynamics.

3˙3. *Effects of the incompressibility K_0.* – The right panel of fig. 3 shows the results corresponding to three EoS with different incompressibilities. For $K_0 = 200$ MeV the system gets quasifission, whereas fusion is observed for the other two larger K_0 values (the compressibility of SAMi-J31 is $K_0 = 245\,\mathrm{MeV}$). The observed dependence of the results on the incompressibility is related to the fact that it is more difficult to compress or to expand the composite reaction system formed along the reaction path, if K_0 is large.

3˙4. *Effects of the isoscalar effective mass m_s^*.* – The effect of the isoscalar effective mass on the quadrupole moment evolution of the reaction considered is shown in fig. 4 (left), by considering parametrizations with larger effective mass than the value associated with SAMi-J31. One can see that, starting from a situation where fusion is observed (SAMi-J31), the increase of the nucleon effective mass does not change the reaction dynamics; however the calculations corresponding to larger effective mass values lead to more compact configurations, associated with a smaller quadrupole moment. In panel (b), we explore the impact of the isoscalar effective mass also on a trajectory leading to quasifission (corresponding to the parametrization Gs35). In this case, it is observed that a larger effective mass changes the reaction dynamics, leading to fusion. In the latter case, the quadrupole evolution exhibits the same pattern in the left panels (a) and (b). To understand these results, one may consider that particles having a smaller effective mass can move faster in the nuclear potential, so that for the system it is easier to escape from the attractive nuclear interaction and evolve towards quasifission. One can also argue that particles with a small isoscalar effective mass can invert more easily their direction of motion, helping the system expansion. On the other hand, a larger
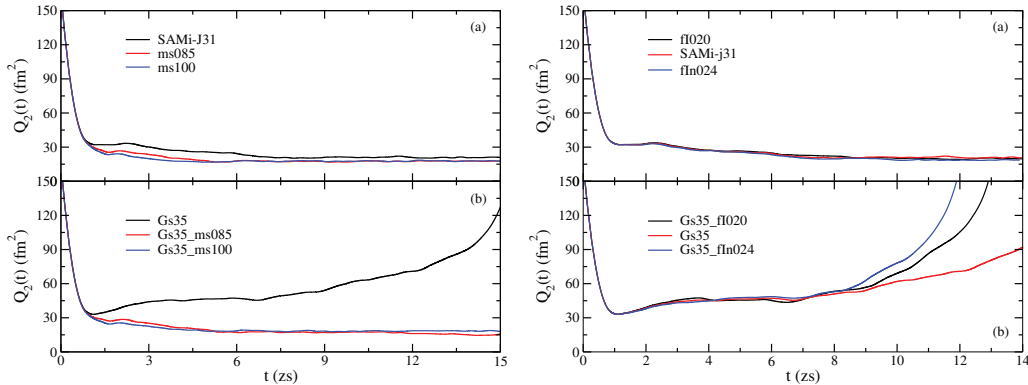
Fig. 4. – Left panels: the dependence of the quadrupole moment evolution on the isoscalar effective mass. Same reaction system as in fig. 1. Right panels: the f_I dependence of the quadrupole moment evolution of the system considered. All reactions are performed at $E_{cm} = 203$ MeV and $b = 0$ fm.

effective mass favors the trapping of the system into the nuclear potential, leading to fusion.

3˙5. *Effects of fI*. – We now concentrate on the reaction dynamics associated with the three EoS having different values of f_I (fig. 4, right panels), adopting the isoscalar surface term of SAMi-J31, (a), and of SAMi-J35, (b). One can observe that the system ends up with fusion for the three cases in panel (a) and quasifission for the three cases in panel (b). Thus the f_I parameter does not affect crucially the outcome of the reaction, either fusion or quasifission. The ordering observed in the right panel (b) may result from a delicate balance between symmetry energy, n/p effective mass splitting and Coulomb repulsion effects. Increasing the neutron-proton effective mass splitting, with $m_n^* < m_p^*$ ("fI020" case), leads to a larger neutron repulsion, in addition to symmetry energy effects. As a result, we observe a faster quasifission dynamics. On the other hand, a n/p effective splitting of opposite sign, with $m_p^* < m_n^*$ ("fIn024" case), tends to counterbalance symmetry energy effects. However, in this situation, the relative role of the Coulomb repulsion is enhanced, that may also lead to a faster dynamics.

4. – Conclusions

To summarize, we have investigated, by employing a variety of effective interactions within the TDHF approach, the impact of several EoS ingredients on the exit channel (fusion *vs.* quasifission) of nuclear reactions at energies close to the Coulomb barrier. In particular, we build up explicit relations between the coefficients of the Skyrme interaction and relevant nuclear properties, such as incompressibility, symmetry energy, effective mass, Lane potential derivative and surface terms, in some analogy with the studies of ref. [16]. We consider EoS mainly differing by one ingredient, with respect to a reference case, to focus on the effect of that particular ingredient on the reaction process. In such a way, we are able to decouple possible correlations among the different sectors of the EoS. The trajectory of the reaction is traced by evaluating the quadrupole moment $Q_2(t)$ of the composite system or by looking at the density contour plots. Calculations are shown for the reaction ^{238}U + ^{40}Ca at $E_{cm} = 203$ MeV and zero impact parameter.

We observe that all the ingredients listed above contribute to the competition between fusion and quasifission processes, however the leading role in determining the outcome of the reaction is played by incompressibility, symmetry energy and the isoscalar coefficient of the surface term. These results enable us to establish possible connections between the reaction dynamics and global nuclear matter properties, opening the perspective to learn on specific aspects which are still poorly known.

<p align="center">∗ ∗ ∗</p>

REFERENCES

[1] SCHRÖDER W. U. and HUIZENGA J. R., *Treatise on Heavy-Ion Science*, edited by BROMLEY D. A. (Plenum, New York) 1984.
[2] LACROIX D., AYIK S. and CHOMAZ P., *Prog. Part. Nucl. Phys.*, **52** (2004) 497.
[3] SIMENEL C., AVEZ B. and LACROIX D., *Quantum Many-Body Dynamics: Applications to Nuclear Reactions* (VDM Verlag, Sarrebruck) 2010.
[4] HINDE D. J. *et al.*, *Phys. Rev. C*, **97** (2018) 024616.
[5] LAZAREV Y. A. *et al.*, *Phys. Rev. Lett.*, **75** (1995) 1903.
[6] OGANESSIAN Y. T. *et al.*, *Phys. Rev. Lett.*, **83** (1999) 3154.
[7] FRÖBRICH P. and LIPPERHEIDE R., *Theory of Nuclear Reactions* (Oxford University Press, New York) 1996.
[8] YILMAZ B., AYIK S., LACROIX D. and YILMAZ O., *Phys. Rev. C*, **90** (2014) 024613.
[9] OBERACKER V. E., UMAR A. S. and SIMENEL C., *Phys. Rev. C*, **90** (2014) 054605.
[10] SIMENEL C., *Eur. Phys. J. A*, **48** (2012) 152.
[11] WAKHLE A. *et al.*, *Phys. Rev. Lett.*, **113** (2014) 182502.
[12] ZHENG H., BURRELLO S., COLONNA M. and BARAN V., *Phys. Lett. B*, **769** (2017) 424.
[13] ZHENG H., BURRELLO S., COLONNA M. and BARAN V., *Phys. Rev. C*, **94** (2016) 014313.
[14] REINHARD P. J., UMAR A. S., STEVENSON P. D., PIEKAREWICZ J., OBERACKER V. E. and MARUHN J. A., *Phys. Rev. C*, **93** (2016) 044618.
[15] SKYRME T. H. R., *Philos. Mag.*, **1** (1956) 1043; *Nucl. Phys.*, **9** (1959) 615; *Nucl. Phys.*, **9** (1959) 635.
[16] CHEN L. W., KO C. M., LI B. A. and XU J., *Phys. Rev. C*, **82** (2010) 024321.
[17] ROCA-MAZA X., COLÒ G. and SAGAWA H., *Phys. Rev. C*, **86** (2012) 031306(R); ROCA-MAZA X. *et al.*, **87** (2013) 034301.
[18] UMAR A. S., OBERACKER V. E. and SIMENEL C., *Phys. Rev. C*, **92** (2015) 024621.
[19] ZHENG H., BURRELLO S., COLONNA M. *et al.*, *Phys. Rev. C*, **98** (2018) 024622.